Myosin V spatially regulates microtubule dynamics and promotes the ubiquitin-dependent degradation of the fission yeast CLIP-170 homologue, Tip1

Rebeca Martín-García and Daniel P. Mulvihill*

School of Biosciences, University of Kent, Canterbury, Kent CT2 7NJ, UK

*Author for correspondence (D.P.Mulvihill@kent.ac.uk)

Accepted 17 August 2009
Journal of Cell Science 122, 3862-3872 Published by The Company of Biologists 2009
doi:10.1242/jcs.054460

Summary

Coordination between microtubule and actin cytoskeletons plays a crucial role during the establishment of cell polarity. In fission yeast, the microtubule cytoskeleton regulates the distribution of actin assembly at the new growing end during the monopolar-to-bipolar growth transition. Here, we describe a novel mechanism in which a myosin V modulates the spatial coordination of proteolysis and microtubule dynamics. In cells lacking a functional copy of the class V myosin, Myo52, the plus ends of microtubules fail to undergo catastrophe on contacting the cell end and continue to grow, curling around the end of the cell. We show that this actin-associated motor regulates the efficient ubiquitin-dependent proteolysis of the *Schizosaccharomyces pombe* CLIP-170 homologue, Tip1. Myo52 facilitates microtubule catastrophe by enhancing Tip1 removal from the plus end of growing microtubules at the cell tips. There, Myo52 and the ubiquitin receptor, Dph1, work in concert to target Tip1 for degradation.

Supplementary material available online at
http://jcs.biologists.org/cgi/content/full/122/21/3862/DC1

Key words: CLIP-170, Dph1, *Schizosaccharomyces pombe*, Class V myosin, Ubiquitin-dependent proteolysis

Introduction

Determination and maintenance of a specific shape is crucial for all cells, as it affects their ability to respond to the external environment. Polar growth determines shape generation in a variety of cell types including neurons, epithelial cells and yeast (Drubin and Nelson, 1996; Hayles and Nurse, 2001; Solomon and Zurn, 1981). Cells must break symmetry to acquire polarity, which is often achieved through cooperation between the actin and microtubule cytoskeletons. This brings about an asymmetric distribution of organelles and polarity factors within the cell to promote the establishment of a polarised pattern of cell growth. The fission yeast *Schizosaccharomyces pombe* is an excellent and simple model organism in which to study how cell shape and polarity are established and maintained. These polarised rod-shaped cells grow exclusively at their cell tips in a spatially and cell-cycle regulated manner.

Newly divided fission yeast cells grow exclusively at the cell end that existed prior to the preceding cell division (the old end). At a specific point during the subsequent G2 period of the cell cycle, a switch to bipolar growth is triggered in an event known as 'new end take off' (NETO). Growth then continues in a bipolar manner until the cell enters mitosis (Mitchison and Nurse, 1985). This transition from monopolar to bipolar growth is reflected in a corresponding change in the actin distribution (Marks et al., 1986). F-actin concentrates to cortical actin patches at regions of cell growth and to actin filaments, which extend towards the cell interior. These actin filaments serve as tracks upon which myosin-V motor proteins mediate the delivery of secretory vesicles and other cellular cargoes to sites of cell growth.

Although actin is essential for polar growth, it is not sufficient to establish a bipolar growth pattern during NETO, which also requires the activity of the microtubule cytoskeleton. In fission yeast, interphase microtubules are arranged within three or four pairs of anti-parallel microtubules, which extend along the longitudinal axis of the cell. Upon nucleation from microtubule-organising centres, each anti-parallel pair of microtubules polymerise, extending the plus ends of microtubules outwards toward the cell tips. In the majority of cases, microtubules undergo catastrophe on reaching the cell cortex at the ends of the cells. In fission yeast, spatial organisation of microtubule dynamics are regulated in part by the action of the microtubule plus-end tracking proteins (+TIPs) Mal3, Peg1 and Tip1, which are homologues of the metazoan EB1, CLASP and CLIP-170 proteins, respectively (Beinhauer et al., 1997; Bratman and Chang, 2007; Brunner and Nurse, 2000; Grallert et al., 2006).

During the transition from monopolar to bipolar growth, microtubules promote actin assembly at the new growing end. Tea1 is a landmark protein that is transported on the plus ends of microtubules and is deposited at the ends of the cell, where it plays an important role in the initiation of a second site of growth (Mata and Nurse, 1997). There, another polarity factor, Tea4/Wsh3, which is also targeted to sites of growth by growing microtubules, associates in a complex with Tea1 (Martin et al., 2005; Tatebe et al., 2005) and together they recruit the formin, For3, to the cell end to promote actin assembly and polarised cell growth (Martin et al., 2005). Then, motor proteins, including class V myosins, regulate the polarised transport of vesicles and other cargoes towards the growing cell tip. Class V myosins are processive actin-associated motor proteins that dimerise to transport molecular cargos throughout the cell (Mehta et al., 1999). Although class V myosins have been demonstrated to play key roles in many diverse cellular processes, the molecular mechanisms by which they undertake these functions in many cases are still unknown. Myo52, one of two

fission yeast class V myosins, travels upon actin filaments and concentrates at sites of cell growth, where it has been implicated to be involved in a number of cellular events including coordinating polarised growth, cytokinesis and vacuole fusion (Motegi et al., 2001; Win et al., 2001).

Recent studies have suggested that ubiquitin-dependent proteolysis plays an important role in the spatial and temporal regulation of polarised cell growth. Indeed, many microtubule- and actin-associated proteins have been reported to be targets for proteasome-dependent degradation (David et al., 2002; Hitchcock et al., 2003; Iioka et al., 2007; Peth et al., 2007). The ubiquitin-proteasome pathway is a conserved complex protein degradation system, which controls many cellular processes such as cell-cycle progression, endocytosis and DNA repair. The variety of cellular functions regulated by ubiquitylation requires that the ubiquitylation machinery is highly substrate-specific and that there exist diverse proteins, interacting with ubiquitylated substrates, that mediate these specific interactions. The ubiquitin-associated (UBA) and ubiquitin-like (UBL) domain proteins constitute one of the best-characterised family of ubiquitin-interacting proteins, and it has been suggested that they shuttle ubiquitylated substrates to the proteasome for degradation (Hartmann-Petersen et al., 2003a; Kang et al., 2006; Rao and Sastry, 2002). Ubiquitin-dependent proteolysis has been established as playing key roles in regulating cell-cycle progression through the modulation of CDK activity, and in regulating chromosome cohesion (Reed, 2003; Reed, 2006). However, little is known about how proteasome-dependent degradation is directly involved in the establishment and maintenance of cell polarity.

Here, we describe a novel mechanism in which a class V myosin, Myo52, modulates the spatial coordination of microtubule dynamics and regulates the efficient ubiquitin-dependent proteolysis of the *S. pombe* CLIP-170 homologue, Tip1. Myo52 facilitates microtubule catastrophe by enhancing Tip1 removal from the plus end of growing microtubules at the cell tips. Then, Myo52 and the ubiquitin receptor, Dph1, work in concert to target Tip1 for degradation. Our findings indicate the existence of a cross-talk between microtubule and actin cytoskeletons to ensure the correct regulation and maintenance of cell growth and polarization.

Results

Motor activity of myosin V regulates microtubule catastrophe

In an attempt to further explore the functions of Myo52, a genetic screen was established to identify mutations within *myo52* that perturb specific aspects of the functions of this motor protein. Temperature-sensitive *myo52-1* mutants had aberrant septa, but also possessed a bent cell morphology, a phenotype normally associated with microtubule and polarisome defects (Fig. 1A) (Grallert et al., 2006; Sawin and Nurse, 1998; Verde et al., 1995). Sequencing the *myo52-1* allele revealed a single amino acid substitution (D55N) within the Src homology (SH3) region of the motor domain. To establish how this mutation affected the ability of Myo52 to associate with actin, strains in which the 3′ end of *myo52* or *myo52-1* alleles were fused to cDNA encoding for eGFP or tdTomato fluorophores were created. Live-cell imaging confirmed that Myo52 made frequent long-distance cytoplasmic movements and concentrated to non-motile foci at the growing cell tips (Fig. 1B) (Grallert et al., 2007). By contrast, Myo52-1 failed to concentrate to the actin-patch-rich cell tips to the same extent as the wild-type protein and made relatively short and less frequent excursions within the cell (Fig. 1B), suggesting that the D55N mutation reduces the motility of Myo52 and its affinity for actin.

Consistent with studies of *myo52Δ* cells (Motegi et al., 2001; Win et al., 2001), the *myo52-1* allele had no effect on the organisation of the actin cytoskeleton after two hours of incubation at the non-permissive temperature (Fig. 1C), at which time the mutant phenotype was observed. However, after extended incubation (>4 hours) at the non-permissive temperature, aberrant actin rings and septa were observed (not shown), consistent with the report that Myo52 plays an important role during cytokinesis (Mulvihill et al., 2006). Because microtubules are important in establishing a polarised growth pattern and cell shape in fission yeast, we next examined the microtubule cytoskeleton in this mutant and discovered that *myo52-1* cells possessed abnormal microtubule dynamics. In this mutant, microtubule plus ends remained in contact with the cell end for twice as long as in equivalent wild-type cells (Table 1). In addition, a large proportion (46%) of the microtubules in *myo52-1* cells failed to undergo catastrophe. Instead, these microtubules continued to grow after contacting the cortex at the cell tip, curling around the end of the cell (Fig. 1D-F; Table 1), a phenomenon that was never seen in wild-type cells containing this *gfp-atb2* allele (this study) (Grallert et al., 2006). These data indicate that the bent cell morphology phenotype seen in *myo52*-1 cells is brought about by the failure of this myosin V to concentrate at the cell poles, where it appears to play a novel role in regulating microtubule dynamics.

Myosin V regulates localisation of CLIP-170

To explore how this myosin affects microtubule dynamics and cell polarity in fission yeast, the localisation of a number of microtubule +TIPs and cell polarity determinants was examined and quantified in strains lacking functional Myo52 (Table 2). Examining the localisation of Tea1 (Mata and Nurse, 1997), Tea2 (Kinesin) (Browning et al., 2000), Mal3 (EB1 homologue) (Beinhauer et al., 1997), or Tip1 (a CLIP-170 homologue) (Brunner and Nurse, 2000) simultaneously in *myo52*$^{+}$ and *myo52-1* cells revealed an intriguing finding. Tea1, a cell polarity determinant, and Tea2, a kinesin in part responsible for its delivery to the ends of polymerising microtubules (from which they are deposited at the cell tips), localised normally in the absence of functional Myo52 (Fig. 2A,B). Similarly the dynamic localisation of Mal3, a microtubule +TIP required for preventing premature microtubule catastrophe (Beinhauer et al., 1997), appeared unaffected in *myo52-1* cells (Fig. 2C) and continued to localise to microtubule plus ends (supplementary material Movie 1). However, Tip1, a microtubule +TIP that controls the spatial regulation of microtubule catastrophe onset (Brunner and Nurse, 2000; Busch and Brunner, 2004), was localised to microtubule ends but failed to localise efficiently to the cell tip in the absence of functional Myo52 (Fig. 2D; supplementary material Movie 2). This was associated with an increased cytoplasmic signal in cells lacking Myo52 when simultaneously compared with *myo52*$^{+}$ cells (supplementary material Movie 2). Myo52 localisation was unaffected in cells lacking Tea1, Tea2, Mal3 or Tip1 (not shown), indicating that although Myo52 affects Tip1 localisation, its own recruitment to the cell tips is independent of these cell polarity factors.

We examined the timing of microtubule Tip1 detachment in relation to the onset of microtubule catastrophe in *tip1-tdTomato gfp-atb2* cells. Time-lapse images revealed that although Tip1 removal from the microtubule plus end is not a prerequisite for catastrophe to occur, its detachment from the microtubule plus end was always seen to precede the onset of microtubule catastrophe at the cell tip (Fig. 3A; supplementary material Movie 3), which

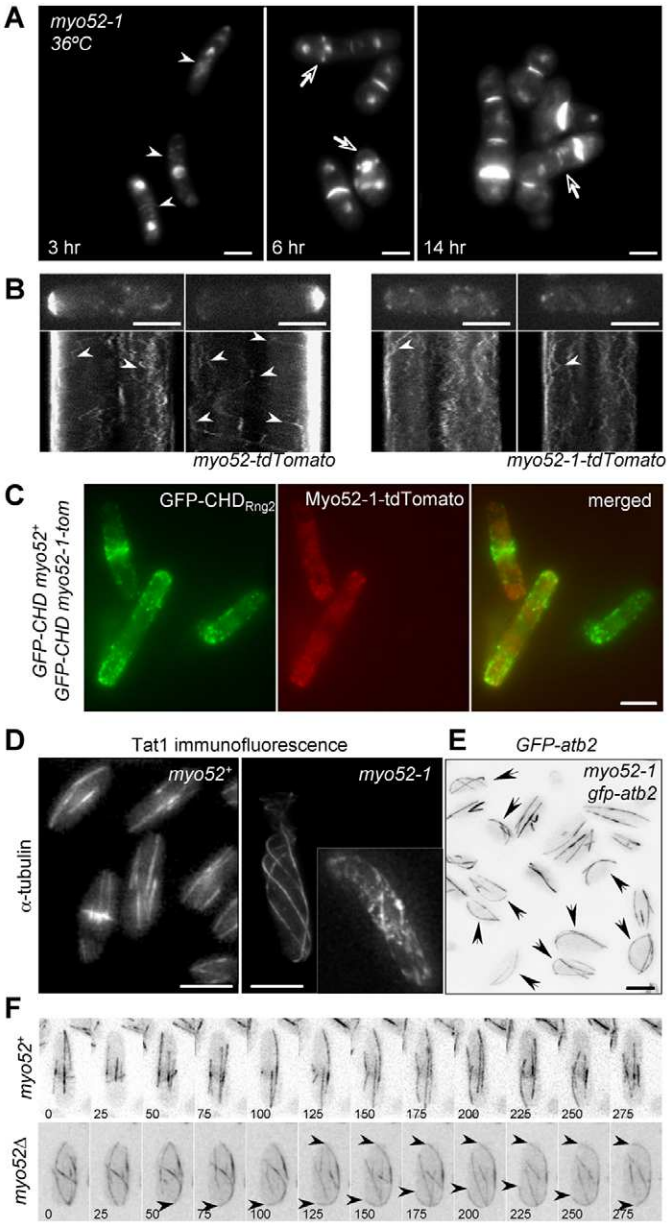

Fig. 1. Myosin V regulates microtubule catastrophe in fission yeast. (A) DAPI and calcofluor staining of DNA and cell walls in *myo52-1* cells incubated at 36°C for 2, 6 and 14 hours reveal defects that include a bent cell morphology (arrowheads), cytokinesis through nuclei (arrows) and multi-septate cells. (B) Micrograph and kymographs of 100 × 100 millisecond timelapse frames of *myo52-tomato* (left) and *myo52-1-tomato* (right) cells illustrate that in contrast to Myo52, Myo52-1 fails to concentrate to the cell tip or to make long distance cytoplasmic movements (arrowheads) to the same extent as the wild-type protein at 36°C. (C) Actin distribution in simultaneously compared in *myo52*$^{+}$ and *myo52-1-tdTomato* cells after incubation at 36°C for 4 hours as revealed by the localisation of GFP-labelled Rng2 calponin homology domain. Actin remains polarised to the ends of growing cells in both cell types. (D) α-tubulin staining (Tat1 immunofluorescence) of *myo52*$^{+}$ and *myo52-1* cells incubated at 36°C for 4 hours. Only *myo52-1* cells have a bent cell morphology and possess bent microtubules (arrows) that have failed to undergo catastrophe. (E) Inverted maximum projection of GFP signal reveals that 46% of *myo52-1 gfp-atb2* cells grown at 36°C for 4 hours possess bent microtubules (arrows). (F) Microtubule dynamics were studied in *myo52*$^{+}$, *myo52Δ* and *myo52-1* cells using an integrated *gfp-atb2* allele under the control of the *nmt81* promoter. Whereas curling microtubules were never seen at the ends of wild-type cells using this allele, microtubules failed to undergo catastrophe and curled upon reaching the cell ends in cells lacking functional Myo52. Each montage shows maximum projections from 21 *z*-serial sections (2 μm apart) corresponding to time frames separated by 25 seconds. Scale bars: 5 μm.

was confirmed in kymographs of *tip1-gfp myo52*$^{+}$ cells (Fig. 3B). In contrast to *myo52*$^{+}$ cells, in which Tip1 foci were almost exclusively seen to travel out to the cell poles before disappearing (Fig. 3B), Tip1 was often seen moving towards the cell centre, even after contacting the cell tip (Fig. 3C). To test whether the curling microtubule phenotype observed in *myo52* mutants was due to a defect in Tip1 release from the microtubule upon contact with the cell pole, live-cell imaging of *myo52Δ tip1-tdTomato gfp-atb2* and *myo52-1 tip1-tdTomato gfp-atb2* cells was undertaken. The images revealed that in the absence of functional Myo52, Tip1-loaded microtubules often continued to grow after reaching the cell end (Fig. 3C), curling around it and extending back into the cell (Fig. 3D; supplementary material Movies 4 and 5). To exclude the possibility that the fluorophore tags affected these dynamics, the presence of Tip1-loaded curling microtubules in *myo52* mutants was confirmed by simultaneous tubulin and Tip1 immunofluorescence staining (not shown). These data suggest that on microtubule contact with the cell tip, myosin V facilitates the efficient detachment of Tip1 from the end of microtubules and its subsequent association with the cell cortex, thus providing a mechanism for regulating the spatial organisation of microtubule catastrophe. Consistent with this idea, Tip1 and the cargo-binding tail domain of Myo52 were able to co-immunoprecipitate, indicating that both proteins might physically interact within the cell (Fig. 4A).

Myo52 prevents Tip1 accumulation at growing cell ends

During periods of monopolar cell growth, components of the polarisome and actomyosin cytoskeleton localise to opposite cell poles, with Myo52 associating with actin at the growing end of the cell and Tip1 being recruited to the non-growing cell tip (Martin et al., 2005). We decided to explore how Myo52 affects Tip1 association with the cell pole. Using the *cdc10-v50* allele to arrest the yeast cell cycle at a point before the switch from a monopolar to bipolar pattern of cell growth, we discovered that Tip1 was delivered along the MT to both cell tips, but failed to accumulate at the actomyosin-rich growing cell end (Fig. 4B; Table 2). This is consistent with a model in which Myo52 is involved in regulating Tip1 levels at the poles. Intriguingly, when we examined Tip1 localization during monopolar growth in *cdc10-v50*-arrested cells lacking Myo52, Tip1 also accumulated to the growing end of cells (Fig. 4B; Table 2). These cells not only failed to elongate as much as equivalent *cdc10-v50 myo52*$^{+}$ cells but also possessed a bent cell morphology, which is probably a consequence of defects in microtubule organisation. These results suggest that, in addition to enhancing Tip1's release from microtubules and attachment to the cortex at sites of cell growth, the presence of Myo52 regulates Tip1 levels at the growing cell tip.

Tip1 undergoes ubiquitylation and proteolysis

Mammalian microtubule +TIPs not only undergo dynamic exchange on microtubule plus ends (Dragestein et al., 2008), but cellular levels of the mammalian Mal3 homologue, EB1 have also been shown to be regulated by ubiquitin-dependent proteolysis (Peth et al., 2007). In this study using the fission yeast *S. pombe*, the build up of cytoplasmic Tip1-GFP signal in *myo52Δ* and *myo52-1* cells (Fig.

Table 1. Microtubule data of strains used in this study

Strain	Number of cells with curling microtubules[a] (%)	Average period of microtubule contact with cell tip[a,b] (seconds)	Average number of microtubules/cell[a]
Wild type	0	24.5±7.9	3.1
myo52-1	46	47.5±17	4.2
myo52Δ	36	42.3±21	3.9
dph1Δ	4	31.6±9.2	3.4
myo52Δ dph1Δ	58	53.3±18.1	4.5

[a]Calculated from microtubules found within >300 cells.
[b]Values are means ± s.d.

2D; supplementary material Movie 2), together with the result observed in *cdc10-v50 myo52Δ* pre-NETO cells, suggest that the +TIP protein levels might not be regulated correctly in the absence of functional Myo52. In addition, the presence of multiple PEST sequences within Tip1 (Brunner and Nurse, 2000) indicates that this protein might be subject to proteolysis. Indeed, abolition of protein synthesis by treatment with cycloheximide (CHX) resulted in a reduction of Tip1 levels (Fig. 5A). This reduction was not only abolished in the *mts3-1* proteasome mutant (Gordon et al., 1996) (Fig. 5B), but was significantly reduced in cells lacking Myo52 (Fig. 5C). The half-life observed for the Tip1 protein (~3 hours) was longer than expected for a protein undergoing regulated proteolysis. Because this might be due to an effect of using CHX, we examined Tip1 levels in a strain in which it was possible to rapidly and specifically inhibit Tip1 expression. Repression of *tip1*$^+$ transcription from the *nmt81* promoter caused Tip1 levels to rapidly decrease (Fig. 5D) in a proteasome-dependent manner (Fig. 5E). Tip1 was calculated to have a half life of ~50 minutes (Fig. 5F), which is similar to the half life of 40 minutes that we observed for Rum1, a protein that is known to undergo rapid cell-cycle proteolysis (Fig. 5F,G) (Benito et al., 1998).

Ubiquitylation is a common protein modification and promotes the targeting of proteins for proteasome-dependent degradation. Additional slower-migrating Tip1-specific bands were often observed in extracts from cells lacking a functional proteasome (Fig. 5B, arrowhead), suggesting that a population of Tip1 in the cell might be ubiquitylated. Consistent with this hypothesis, anti-hemagglutin (HA) immunoprecipitates from *tip1-HA* cells in which ubiquitin was overexpressed from a pREP1 plasmid (Benito et al., 1998), revealed multiple bands that had lower mobility on SDS-PAGE gels than Tip1-HA alone. The size, number, and intensity of the bands recognised by the HA antibody increased when immunoprecipitations were prepared from cells lacking a functional proteasome (Fig. 5H). In addition, treatment with λ-phosphatase had no affect upon the appearance of these multiple Tip-HA bands (not shown) indicating that they do not correspond to different phospho-forms of Tip1. Together, these data suggest that Tip1 is ubiquitylated and then subject to proteasome-dependent proteolysis, which is enhanced by the activity of the class V myosin, Myo52.

Tip1 and Myo52 associate with the ubiquitin receptor, *Dph1*

During a yeast two-hybrid screen to identify how Tip1 and Myo52 interact with the proteasome, we detected a specific and strong interaction between the tail domain of Myo52 and the ubiquitin receptor, Dph1 (Fig. 6A; supplementary material Fig. S1). This molecule is a member of a conserved class of proteins that contain a ubiquitin-associated (UBA) domain, through which they bind ubiquitylated proteins and target them for proteolysis (Elsasser and Finley, 2005; Hartmann-Petersen et al., 2003b). This physical interaction between Myo52 and Dph1 was confirmed by our ability to co-immunoprecipitate Dph1 with Myo52 tail from fission yeast cells (Fig. 6B). Using yeast two-hybrid analysis, we were also able to detect an interaction between Dph1 and Tip1, consistent with a

Table 2. Signal intensities at cell poles

Strain	Average pole signal normalised to cytoplasm*	Average pole signal normalised to background	Normalised signal at growing pole*	Normalised signal at non-growing pole*
tea1-gfp myo52$^+$	1.55±0.72[a]			
tea1-gfp myo52-1	1.44±0.63[a]			
tea2-gfp myo52$^+$	1.63±0.21[b]			
tea2-gfp myo52-1	1.56±0.18[b]			
tip1-4gfp myo52$^+$	3.15±0.85[c]			
tip1-4gfp myo52-1	1.41±0.52[c]			
tip1-tdTom myo52$^+$	2.07±0.30[d]			
tip1-tdTom myo52-1	1.19±0.48[d]			
tip1-4gfp dph1$^+$	3.27±1.1[e]			
tip1-4gfp dph1Δ	6.33±1.8[e]			
tip1-tdTom myo52$^+$ *dph1*$^+$	1.91±0.43[f]	2.57±0.73[f]		
tip1-tdTom dph1Δ myo52Δ	1.81±0.30[f]	5.13±0.60[f]		
tip1-tdTom cdc10-v50			1.49±0.23	3.42±0.73
tip1-tdTom cdc10-v50 myo52Δ			2.60±0.43	2.54±0.44

*Sample size >50.
[a,b,c,d,e,f]Signals measured from same sample containing mixture of paired cell types. Values are means ± s.d.

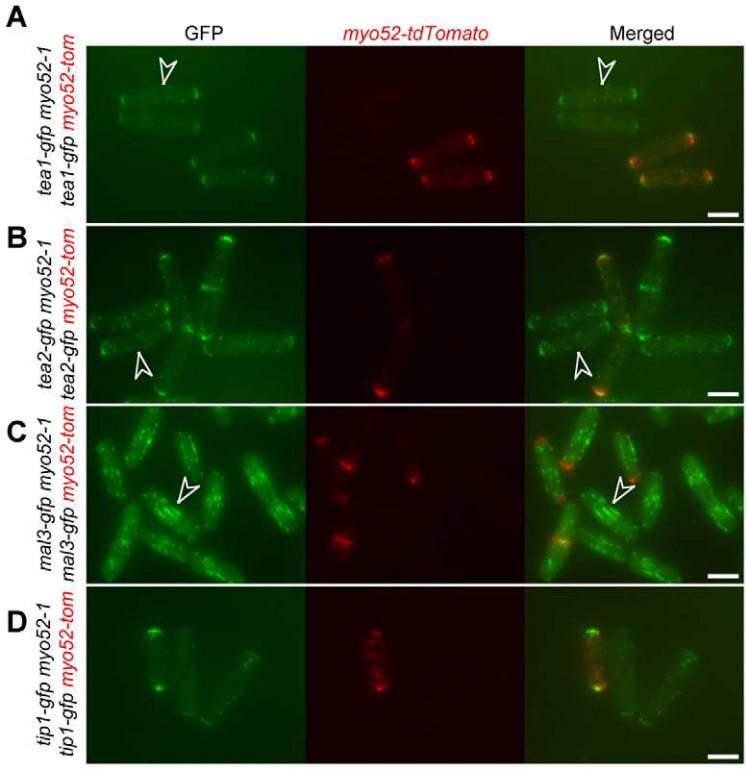

Fig. 2. Myo52 regulates interaction of Tip1 with the cell tip. Localisation of Tea1-GFP (A), Tea2-GFP (B), Mal3-GFP (C) and Tip1-4GFP (D) simultaneously compared in *myo52-tdTomato* and *myo52-1* cells. Whereas GFP signals (green) are equivalent in both backgrounds for Tea1 (A), Tea2 (B) and Mal3 (C), Tip1 recruitment to the cell tips is aberrant in the *myo52* mutant (D). Arrowheads highlight cells with a bent cell morphology. Scale bars: 5 µm.

hypothesis that Dph1 regulates the proteasome-dependent degradation of Tip1. This interaction was dependent upon the UBA domain of Dph1, indicating that Dph1 only associates with Tip1 after ubiquitylation (Fig. 6A; supplementary material Fig. S1). By contrast, the interaction of Dph1 with the tail of Myo52 was independent of its C-terminal UBA domain, which confirms biochemical data (not shown) indicating that Myo52 is not a target for proteolysis (Fig. 6A).

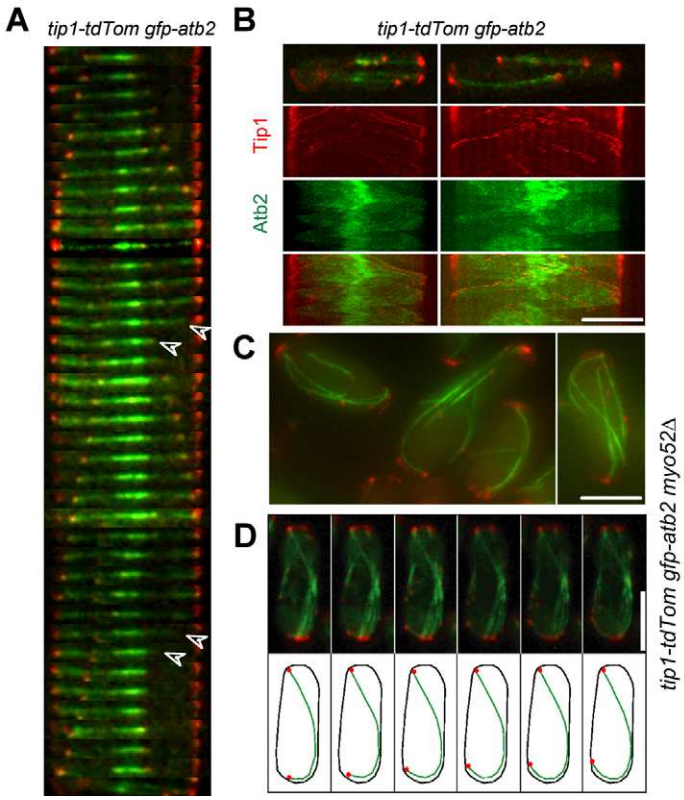

Fig. 3. (A) Kymograph of a microtubule from the timelapse movie of *gfp-atb2 tip1-tdTomato* cells shown in supplementary material Movie 3. Tip1 labels the plus end of polymerising microtubules until contacting the cell tip, when Tip1 is deposited at the cortex and the microtubules undergo catastrophe (highlighted by arrowheads). (B) Kymographs of time frames showing maximum projections from 21 *z*-serial sections of *tip1-gfp tip1-tdTomato* cells illustrate that Tip1 removal from the microtubule tip precedes catastrophe. Time covered by kymographs is 300 seconds each (60× images taken every 5 seconds). (C) Maximum projections of GFP-Atb2 (green) and Tip1-tdTomato (red) localisation in *gfp-atb2 tip1-tdTomato myo52Δ* cells grown at 36°C confirm that Tip1 remains attached to the ends of bent microtubules that failed to undergo catastrophe when reaching the cell end. (D) Consecutive 5-second time-lapse images (upper panels) and diagrammatic representation (lower panels) of *gfp-atb2 tip1-tdTomato myo52Δ* cells demonstrate that Tip1-loaded microtubules continue to grow after contacting the cell end in the absence of Myo52. Scale bars: 5 µm.

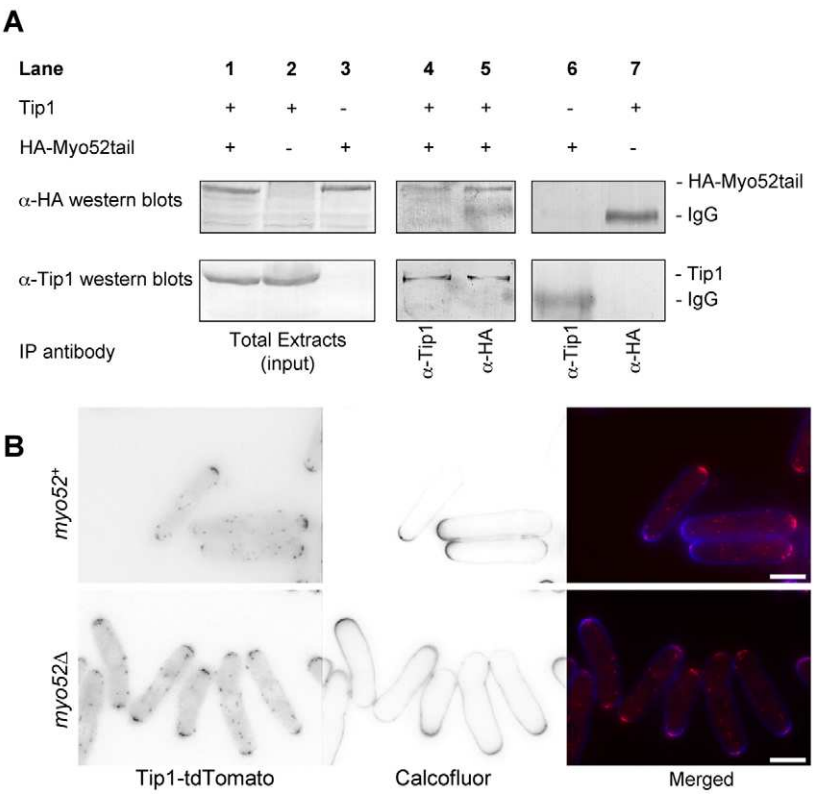

Fig. 4. Myo52 interacts with Tip1 and affects its turnover at the cell pole. (A) Tip1 co-immunoprecipitates with Myo52. Extracts from yeast containing plasmids expressing either Tip1 (lanes 2 and 7), HA-tagged Myo52 tail (lanes 3 and 6) or both Tip1 and HA-Myo52 tail (lanes 1, 4 and 5) were either directly subjected to SDS-PAGE analysis (lanes 1, 2 and 3) or to immunoprecipitations with anti-Tip1 (lanes 4 and 6) or anti-HA antibodies (lanes 5 and 7). Membranes were subsequently probed with anti-HA (upper panels) and anti-Tip1 (lower panels) antibodies. (B) Tip1-tomato localisation (left panels and red in right panels) and calcofluor staining (middle panels and blue in right panels) of *cdc10-v50 myo52*$^{+}$ (upper panels) and *cdc10-v50 myo52Δ* (lower panels) cells arrested in G1 phase of the cell cycle. Whereas Tip1 signal concentrates at the non-growing cell end (upper panels), it accumulates at both cell poles in cells lacking Myo52 (lower panels). As well as highlighting regions of cell growth, calcofluor staining reveals a bent-cell morphology in *cdc10-v50 myo52Δ* cells. Scale bars: 5 μm.

Myo52 and Dph1 modulate Tip1 proteolysis

Overexpression of Dph1 has been reported to bring about microtubule defects (He et al., 1998; Pardo and Nurse, 2005). We discovered that microtubules were sometimes seen to curl around the cell tip in cells lacking Dph1, which occasionally led to a bent cell morphology (Fig. 7A). *dph1Δ* cells also have significantly more Tip1 at the cell end than equivalent wild-type cells (Fig. 7B; Table 2), which indicates that although Dph1 is not required for Tip1 deposition at the cell end, it could be involved in its subsequent removal and degradation.

These data suggest a potential mechanism by which Myo52 associates with Dph1 to target ubiquitylated Tip1 for proteolysis. To confirm this hypothesis, we first examined whether Dph1 affected Tip1 proteolysis by comparing Tip1 levels in *dph1*$^{+}$ and *dph1Δ* cells after treatment with CHX. We discovered that Tip1 degradation is reduced in cells lacking Dph1 (Fig. 7C). Quantification of Tip1 levels in CHX-treated wild-type, *myo52Δ*, *dph1Δ*, *dph1Δmyo52Δ* and *mts3-1* cells revealed that although the rate of Tip1 proteolysis is significantly reduced in cells lacking either Myo52 or Dph1, it is not abolished. However, proteolysis was abolished in *mts3-1* cells, which lack a functional proteasome (Fig. 5B; Fig. 7; supplementary material Fig. S2). Therefore, although both Myo52 and Dph1 are required for normal and efficient Tip1 proteolysis to occur, either protein is capable of promoting Tip1 degradation alone, albeit with significantly reduced efficiency.

As a reflection of the defect in Tip1 degradation in the *dph1Δmyo52Δ* mutant, not only was a significant increase in Tip1-tdTomato signal observed at the tips of these cells, but there was also a significant increase in cytoplasmic Tip1-tdTomato signal, indicating defects in Tip1 proteolysis and also its efficient recruitment to the correct cellular locations in these cells (Fig. 7D; Table 2). Further analysis revealed that a higher proportion of *dph1Δmyo52Δ* cells possess bent microtubules than either of the single deletion strains. In addition, *myo52Δ* and *dph1Δmyo52Δ* cells contain an increased number of microtubules (Table 1; supplementary material Fig. S2) compared to a wild-type strain. Together, these data suggest that Myo52 and Dph1 might act with other as-yet-undefined molecules to influence microtubule organization and dynamics.

Discussion

A number of recent studies have revealed the important role that cross-talk between the microtubule and actin cytoskeletons plays in a number of cellular processes, such as asymmetric cell division, establishment of new cell growth zones and cell migration (Goode et al., 2000; Hwang et al., 2003; Kawasaki et al., 2003; Martin et al., 2005; Wen et al., 2004; Yin et al., 2000). Microtubule dynamics influence the site of actin assembly and cell growth in fission yeast. In this study we describe a novel mechanism in which Myo52, a motor protein associated with the actin of myosin V, spatially regulates microtubule dynamics in fission yeast. These results provide fresh insights into how the interdependent relationship between these two cytoskeletons affects their organisation and functions.

The *myo52-1* mutant, isolated in a screen to identify novel temperature-sensitive *myo52* alleles, possessed a single mutation within the SH3 region of the motor domain. This region has been shown to have an important role in coordinating ATPase activity and actin association in myosins (Fujita-Becker et al., 2006). This is consistent with our observation that at the restrictive temperature the Myo52-1 protein not only failed to concentrate to growing ends of the cell to the same extent as the wild-type protein, but also had a reduced mobility upon actin filaments. Surprisingly, when the *myo52-1* mutant was incubated at the restrictive temperature, a high

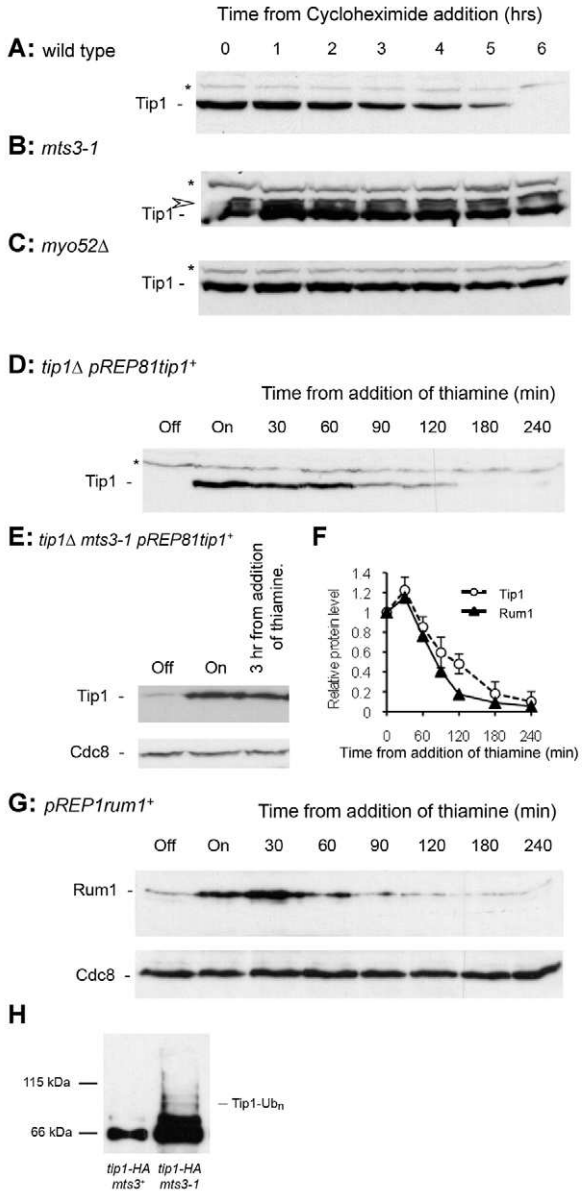

Fig. 5. Tip1 undergoes ubiquitin-dependent proteolysis. Anti-Tip1 western blots of time-course samples from cycloheximide-treated wild-type (A), *mts3-1* (B) and *myo52Δ* (C) cells. Whereas levels of a non-specific cross-reacting band remain constant (*), Tip1 levels decrease in a proteasome-dependent manner. An additional slower-migrating Tip1 band was also observed in extracts from *mts3-1* cells (arrowhead). Anti-Tip1 western blots of time-course samples in which Tip1 expression was switched off in *tip1Δ mts3*$^+$ (D) or *tip1Δ mts3-1* (E) cells, each containing the plasmid pREP81*tip1*$^+$. *tip1*$^+$ transcription from the *nmt* was repressed at time 0 by the addition of thiamine to a concentration of 5 μg/ml. Cells were subsequently incubated at 36°C. (F) Graph showing changes in relative Tip1 (white circles) and Rum1 (black triangles) levels after suppressing *tip1*$^+$ transcription from the *nmt* promoter by thiamine addition. (G) Anti-Rum1 western blots of time-course samples in which Rum1 expression was switched off in cells containing the plasmid *pREP1rum1*$^+$ (as in D). (H) Anti-Tip1 western blot of anti-HA immunoprecipitations from extracts of *mts3*$^+$ and *mts3-1* cells illustrate that Tip1-HA immunoprecipitates as multiple slower migrating isoforms in *mts3-1* cells.

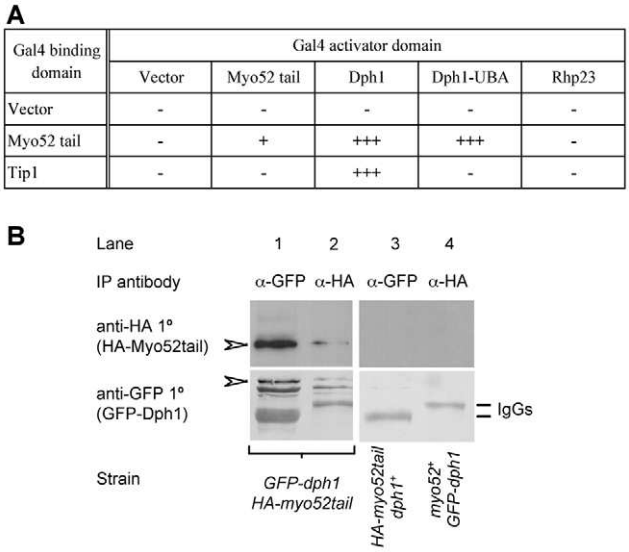

Fig. 6. Myo52 and Tip1 interact with the ubiquitin receptor Dph1. (A) Summary of two-hybrid analysis of interactions between Myo52, Tip1 and the ubiquitin receptor, Dph1. (B) Dph1 coimmunoprecipitates with Myo52. Extracts from yeast expressing either endogenous GFP-tagged Dph1 (lane 4), HA-tagged Myo52 tail (lane 3) or both GFP- Dph1 and HA-Myo52 tail (lanes 1 and 2) were immunoprecipitated with anti-GFP (lanes 1 and 3) and anti-HA antibodies (lanes 2 and 4). Membranes were subsequently probed with anti-HA (upper panels) and anti-GFP (lower panels) antibodies.

proportion of cells possessed microtubules that failed to undergo catastrophe upon reaching the cell cortex at the cell end and instead continued to grow and curl around the cell tip. Bent microtubules were also observed in cells either lacking Myo52, or in which Myo52 localisation and function had been perturbed through the disruption of the actin cytoskeleton (not shown). These data indicate that Myo52 motor activity plays an important role in modulating microtubule dynamics in *S. pombe*.

It has been suggested that it might be necessary for the fission yeast CLIP-170 homologue, Tip1, to be removed from the plus end of a microtubule to ensure that microtubule catastrophe occurs at the end of the cell (Brunner and Nurse, 2000; Busch and Brunner, 2004; Zimmerman and Chang, 2005). Indeed, our findings are consistent with this idea, and although catastrophe can sometimes occur while Tip1 is associated with the microtubule (occurs in ~3% of catastrophe events), when Tip1 reached the cell end it was always seen to detach from microtubules before catastrophe occurred (Fig. 3; supplementary material Movie 3) (Brunner and Nurse, 2000). In addition, this model is consistent with our observation that, in cells lacking functional Myo52, Tip1 fails to recruit normally to the cell tip and instead remains associated with the plus end of microtubules, which subsequently continue to grow after contacting the cell tip and curl around the end of the cell. Indeed these microtubules appear to continue to grow until Tip1 signal is lost from their plus tips (e.g. supplementary material Movies 4 and 5). Therefore, Myo52 appears to promote the spatial regulation of microtubule dynamics by facilitating the detachment of Tip1 from the microtubule plus end and binding to the cell cortex.

In metazoan cells, IQGAP actin-binding proteins serve as recognition targets to allow CLIP-170 to identify the growing cell periphery and also participate in the detachment of CLIP-170 from the plus ends of microtubule (Fukata et al., 2002). The sole fission yeast IQGAP, Rng2, has not been reported to localise at the cell ends (Eng et al., 1998), suggesting that other molecules might have a similar role in *S. pombe*. Is Myo52 one of those molecules? This idea is consistent with our observations that Tip 1 and the tail domain

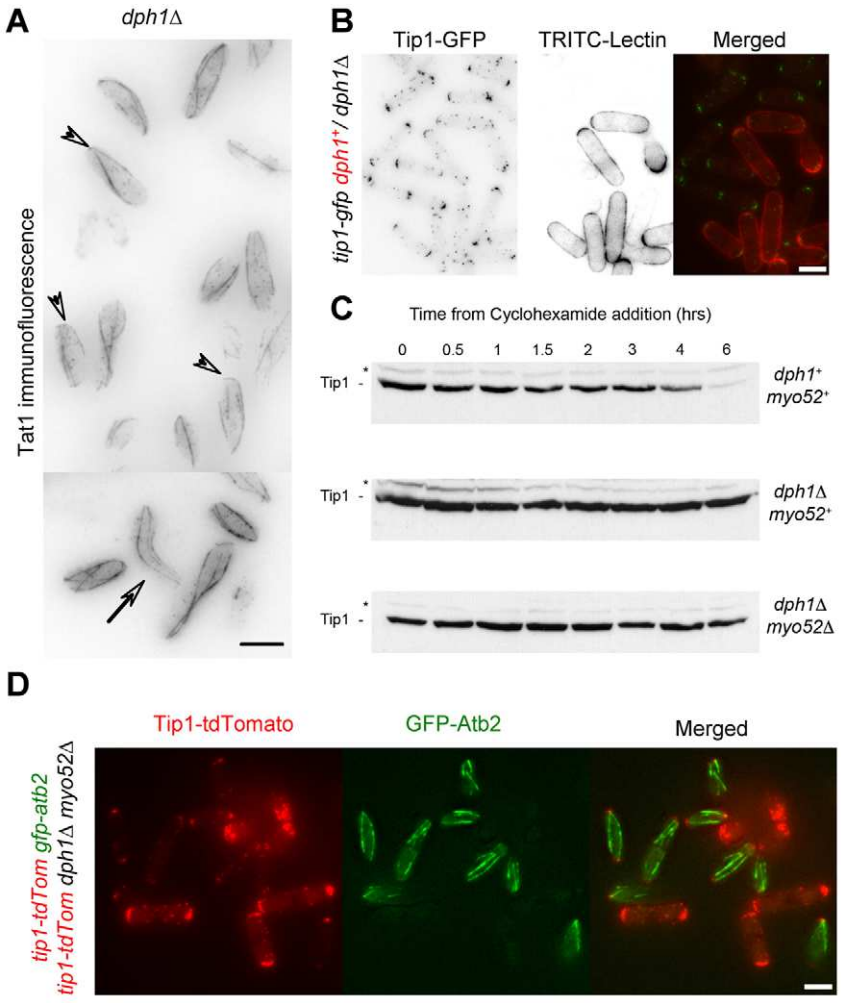

Fig. 7. Myo52 and Dph1 both regulate Tip1 proteolysis. (A) α-tubulin staining of *dph1Δ* cells with Tat1 reveals that a proportion of cells lacking Dph1 have curling microtubules (arrowheads) sometimes associated with a bent cell phenotype (arrow). (B) Localisation of Tip1-GFP (left panel, green in right panel) compared simultaneously in the presence (*dph1*$^{+}$) and absence (*dph1Δ*) of Dph1. *dph1*$^{+}$ cells are identified by TRITC-lectin-coated cell walls (middle panel, red in right panel). (C) Anti-Tip1 western blots of time-course samples from cycloheximide-treated wild-type (upper panel), *dph1Δ* (middle panel) and *dph1Δ myo52Δ* (bottom panel) cells. Levels of non-specific cross-reacting bands (*) remain constant. (D) Localisation of Tip1-tdTomato (left panel, red in right panel) compared simultaneously in wild-type cells expressing GFP–α-tubulin and in *dph1Δmyo52Δ* cells. Wild-type cells are identified by cells containing GFP-labelled microtubules (middle panel, green in right panel). Scale bars: 5 μm.

of Myo52 co-precipitate together and that both microtubule dynamics and Tip1 localization are disrupted in cells lacking functional Myo52. However, as the ability of Tip1 to associate with the polar cell cortex was not completely abolished in cells lacking functional Myo52, it is likely that other factors would be sufficient to bring about Tip1 detachment from the microtubule plus end and subsequent interaction with the cell cortex. This would explain in part the observation that Tip1 is able to accumulate to the non-growing end (where Myo52 is not concentrated) in *cdc10-v50* arrested pre-NETO cells, which also suggests that different polarity or cortical factors might be involved in the spatial regulation of microtubule dynamics during different stages of the cell growth cycle.

An alternative hypothesis to explain how Myo52 regulates localisation of Tip1 is that this class V myosin, which transports cargoes along the actin filaments, might be involved in the delivery to the cell end (and/or maintenance at the cell end) of an as-yet-unknown factor that allows Tip1 to distinctly recognise and attach to the cell cortex at the tip. In the absence of a functional Myo52, those factors could reach the cell tip by other means although with less efficiency (e.g. passive diffusion). Potential myosin-V cargoes could be enzymes that bring about post-translational modifications to induce Tip1 detachment from the microtubule plus end. Indeed, Tip1 is a phosphoprotein (our unpublished data) and phosphorylation has been shown to reduce the affinity of CLIP-170 for microtubules (Rickard and Kreis, 1991). However, at present the role phosphorylation plays in modulating Tip1 activity within fission yeast remains unresolved.

Cortex-associated Tip1 is highly dynamic at growing cell ends (Brunner and Nurse, 2000), indicating the existence of a mechanism to regulate Tip1 attachment and exchange. Consistent with a model in which Myo52 is involved in regulating Tip1 exchange at the cell poles, we observed that the fission yeast CLIP-170 homologue failed to accumulate at the actomyosin-rich growing end of *cdc10-v50* cells arrested in the monopolar growth phase of the cell cycle. In these cells, Myo52 and Tip1 concentrate to opposite poles. The same phenomenon has been observed in cells lacking the polarity determinant Tea4, required for the establishment of bipolar growth (Martin et al., 2005). By contrast, Tip1 accumulated at both growing and non-growing cell ends in *cdc10-v50* arrested cells lacking Myo52. These data indicate that Myo52 is involved in regulating Tip1 exchange or turnover at the cell ends.

How does the Tip1 turnover occur? Is it just due to a change in localization or does it involve protein degradation? The presence of multiple PEST sequences within the Tip1 protein indicates that Tip1 might be turned over by proteolysis. In support of this idea, we detected a reduction of Tip1 levels after the addition of CHX, an inhibitor of protein synthesis. This reduction in Tip1 levels was not as dramatic in *myo52Δ* cells, which is in agreement with the above model in which Myo52 regulates Tip1 turnover at the cell

ends. In addition, after CHX treatment of a proteasome mutant, Tip1 levels remained substantially unchanged, suggesting that Tip1 is subject to proteolysis by the 26S multi-subunit proteasome complex. However, the rate of turnover for this protein after CHX treatment was lower than that observed for other substrates of proteasome degradation (Benito et al., 1998). One explanation is that only a subpopulation of Tip1 is degraded. Alternatively, the rate of Tip1 turnover could be decreased by CHX treatment, as this chemical inhibits protein synthesis globally in the cell (i.e. inhibits the de novo synthesis of proteins involved in cell-cycle progression), which might affect the rate of Tip1 degradation. When we developed *tip1* switch-off experiments, using the repressible *nmt* promoter as an approach to analyse Tip1 degradation rates, we observed a turnover rate similar to those seen for known proteasome substrates such as the Cdk inhibitor, Rum1. Many substrates of the proteasome complex, including Rum1, undergo polyubiquitylation, which targets them for degradation. We determined that Tip1 is subjected to this post-translational modification, and together these data confirm that Tip1 levels are regulated by ubiquitin-dependent proteolysis.

It was unclear how this Myo52-dependent Tip1 proteolysis was regulated. Using a yeast two-hybrid screen we established that the ubiquitin receptor, Dph1, associated with the tail of Myo52 (confirmed by co-immunoprecipitations) and Tip1. Dph1 is a member of a family of UBA-domain-containing proteins that are responsible for the presentation of polyubiquitylated proteins to the proteasome (Wilkinson et al., 1998). We discovered that the conserved UBA domain within the C-terminal of Dph1 is indispensable for its interaction with Tip1 (in contrast to the interaction between Dph1 and Myo52, which is UBA-independent), suggesting that Dph1 targets Tip1 for degradation. In support of this idea, we have shown that whereas Tip1 proteolysis is reduced in *dph1Δ* cells, increased levels of this microtubule +TIP were seen accumulated at their cell tips. These observations indicate that, like Myo52, Dph1 modulates the cellular levels and distribution of Tip1. A proportion of *dph1Δ* cells possessed curling microtubules and had a bent morphology. This is consistent with the previously reported observation that overexpression of Dph1 results in defects in microtubule organisation (He et al., 1998; Pardo and Nurse, 2005). These data suggest a role for Dph1 in regulating microtubule organization and/or dynamics, but at this point is not possible to confirm whether this is related to the degradation of Tip1 or whether these are independent phenomenon.

Although Myo52 and Dph1 are each required for the efficient proteolysis of Tip1 to occur, either protein is capable of promoting Tip1 degradation in the absence of the other, albeit with reduced efficiency. However, Tip1 proteolysis was dramatically reduced in cells lacking both Dph1 and Myo52. This suggests that Myo52 and Dph1 work in concert to efficiently regulate Tip1 turnover. Because the ubiquitin-receptor proteins (family of proteins to which Dph1 belongs) have been described as often having common overlapping substrates (Elsasser and Finley, 2005; Wilkinson et al., 2001), it is possible that other ubiquitin receptors might share a role with Dph1 in regulating Tip1 proteolysis.

Our results suggest a potential mechanism by which Myo52 associates with Dph1 to target ubiquitylated Tip1 for proteolysis. The UBL (ubiquitin-like) domain present in ubiquitin-receptor proteins such as Dph1 has been shown to be essential for their interaction with the 26S proteasome. Thus, we propose a model in which Dph1 binds to ubiquitylated Tip1 to facilitate its rapid degradation. The subsequent proteolysis of Tip1 is likely to require transport of the Tip1-bound Dph1 from the cell ends to the proteasome. Such a process is probably microtubule-independent because Tip1 can still be rapidly turned over at the cell tips after treatment with microtubule depolymerising drugs (Brunner and Nurse, 2000). Although we have detected Myo52 and Tip1 colocalising to foci within the cytoplasm of fission yeast cells, technical limitations have not allowed us to detect both proteins moving together. Using biochemical and yeast two-hybrid methods we have identified a physical interaction between Myo52, Dph1 and Tip1. However, further study is required to uncover the precise mechanism by which Tip1 interacts with the polar cell cortex and how it is subsequently delivered to the proteasome for degradation.

It is intriguing to speculate that myosin-V-dependent regulation of CLIP170 proteolysis might be conserved throughout the animal kingdom. Metazoan processive myosins have been shown to associate with microtubule +TIPS. Mammalian myosin Va associates with both EB1 and melanophilin (Wu et al., 2005), whereas myosin VI associates with CLIP-170 in *Drosophila* neurones and embryos (Lantz and Miller, 1998). This suggests the exciting possibility that the actomyosin cytoskeleton plays a conserved and key role in regulating the spatial organisation of cell polarity determinants and microtubule dynamics to affect cell shape and development.

Materials and Methods

Yeast cell culture and strains

S. pombe strains used in this study are listed in supplementary material Table S1. Cell culture and maintenance were carried out using standard methods (Moreno et al., 1991). Cells were cultured in rich (YES) or minimal (EMM2) supplemented media at 25°C. Temperature-sensitive (ts) *myo52* alleles were isolated using the previously described marker switch technique (MacIver et al., 2003). Full-length ts *myo52* alleles were sequenced to identify changes to the polypeptide sequence. Protein synthesis was inhibited by addition of CHX (Sigma) at a final concentration of 100 μg/ml. To induce the expression from the *nmt1* and *nmt81* promoters, cells were grown in EMM media supplemented with 5 μg/ml thiamine to mid-log phase, washed three times and resuspended in EMM lacking thiamine, at a density calculated to produce 4×10^6 cells/ml after 18 hours of growth. For the *nmt* switch-off experiments, cells were shifted from 25°C to 36°C and thiamine was simultaneously added to a concentration of 5 μg/ml.

Molecular biology

Strains in which the 3′ end of the endogenous *myo52, myo52-1, tip1* or *dph1* alleles were fused to cDNA encoding for either the eGFP or tdTomato fluorophores or the HA epitope were created as described previously using the appropriate template (Bahler et al., 1998) and primers (supplementary material Table S2). The Gal4-binding domain (BD) vectors pGBKT7 and pGBDU, and the Gal4-activating domain (AD) vectors pGADT7 and pGADGH (Clontech) were used in yeast two-hybrid experiments. DNA encoding Dph1 and Dph1-UBA were amplified from fission yeast genomic DNA (using the o282, o283 and o284 oligos respectively), sequenced and ligated into the *Nde*I-*Bam*HI sites of pGADT7 to create pGADT7*dph1*, pGADT7*dph1-UBA*. *tip1*$^+$ and *rum1*$^+$ constructs were created by PCR amplification from cDNA (using the o266, o270, o297 and o298 oligos, respectively) containing the *Nde*I and *Bam*HI flanking restriction sites, and cloned into pGEM. The *Nde*I-*Bam*HI fragments from pGEM-*tip1*$^+$ and pGEM-*rum1*$^+$ were subcloned into pET28a, pREP81 and pREP1 to create pET28a-*tip1*$^+$, pREP81*tip1*$^+$ and pREP1*rum1*$^+$.

Antibody production

pET28a-*tip1*$^+$ plasmid was introduced into BL21 cells, Tip1 expression was induced and the full-length recombinant Tip1 was purified from inclusion bodies using established techniques (Harlow and Lane, 1988). Antibodies were raised against the purified Tip1 protein in SPF rabbits (Eurogentec, Liege, Belgium) and were subsequently affinity-purified using Pierce AminoLink Plus Immobilisation columns (Pierce).

Yeast protein extracts

Yeast protein extracts were prepared from 6×10^7 cells collected by centrifugation, washed in cold STOP buffer (Simanis and Nurse, 1986) and resuspended in 100 μl of yeast protein extraction (YPE) buffer (50 mM HEPES pH 8.0, 200 mM KCl, 5 mM EDTA, 5 mM EGTA, 50 mM NaF, 50 mM sodium-β-glycerophosphate, 0.1% v/v Triton X-100 supplemented with the following protease inhibitors: 1 μg/ml AEBSF, 1 μg/ml antipain, 1 μg/ml aprotinin, 10 μM benzamidine, 1 μg/ml

chymostatin, 1 μg/ml E64, 1 μg/ml leupeptin, 1 μg/ml pepstatin, 5 μM phenanthroline, and 1 mM PMSF). Cells were disrupted by mechanical lysis using a Fastprep FP120 (Bio101 Thermo Savant). For immunoprecipitation involving Myo52- and Dph1-tagged proteins, the YPE buffer was modified by addition of 1% (v/v) Triton X-100, 5 mM ATP and 5 mM $MgCl_2$. Total yeast extracts were centrifuged at 3000 ***g*** for 5 minutes to remove cells debris, then mixed with SDS-PAGE loading buffer and boiled for 5 minutes before analysis by SDS-PAGE. Extracts used to analyse Rum1 levels were prepared using established methods (Benito et al., 1998).

Immunoprecipitations

Protein-A-Sepharose beads pre-bound to appropriate antibodies were added to microfuge tubes containing equal quantities of cleared yeast extracts. Immuno-complexes were subsequently washed four times in 100 μl of YPE buffer, resuspended and boiled in an equal volume of 2× SDS-PAGE loading buffer.

Western blotting

Anti-HA (12CA5, Roche) and *anti-GFP* (3E1, a generous gift from Iain Hagan, University of Manchester, Manchester, UK and William Gullick, University of Kent, Canterbury, UK) monoclonal antibodies were used at 1:5000 and 1:1000 dilutions, respectively. Cdc8 and Tip1 levels were detected using 1:1000 dilutions of this labaratory's affinity-purified *anti-Cdc8* and *anti-Tip1* polyclonal antibodies. Peroxidase-conjugated secondary antibodies and SuperSignal West Pico chemiluminescent substrate (Pierce Biotechnology) were used for antibody detection in the experiments shown in Figs 4-7. Alkaline-phosphatase-conjugated secondary antibodies together with NCBPIP substrate (Sigma, UK) were used for quantification of proteins because this detection method gives a linear relationship between signal and quantity of protein. Western blot membranes were digitised using an Epson Perfection V750 Pro scanner, and signal intensities were subsequently determined using ImageJ software (http://rsb.info.nih.gov/ij/; NIH, Bethesda, MA). The changes in Tip1 levels were normalised against a control protein (e.g. Cdc8). Each experiment was repeated at least three times to confirm the results. Relative protein levels obtained from each experiment were averaged and are shown in supplementary material Fig. S2.

Microscopy

Samples were visualised using an Olympus IX71 microscope with PlanApo 100× OTIRFM-SP 1.45 NA lens mounted on a PIFOC *z*-axis focus drive (Physik Instrumente, Karlsruhe, Germany), and illuminated using an automated 300 W Xenon light source (Sutter, Novato, CA) with ET-sedat filters (Chroma, Bellows Falls, VT). Samples were visualised via a QuantEM CCD camera (Photometrics) and the system was controlled with Metamorph software (Molecular Devices). Each 3D-maximum projection of volume data was calculated from 21 *z*-plane images, each 0.2 μm apart, using Metamorph or Autoquant X software. During live-cell imaging, cells were mounted onto coverslips with lectin (Sigma L2380; 1 mg/ml) in a Bioptechs FCS2 (Bioptechs, Butler, PA), fitted onto an ASI motorised stage (ASI, Eugene, OR) on the above system, with the sample holder, objective lens and environmental chamber held at the required temperature. All live-cell imaging was undertaken using EMM2 media supplemented with appropriate amino acids. Standard immunofluorescence procedure using TAT1 (anti α-tubulin) antibody was as described previously (Hagan and Hyams, 1988). Microtubules were analysed from fluorescence images and were defined to have a bent morphology if the end pointed inward into the cell. For each genotype, at least 300 microtubules were counted to determine average time of contact at the cell poles (expressed as mean ± s.d.) and more than 300 cells to determine the frequency occurrence of curled phenotype and to count the number of microtubules and/or bundles. This data is summarised in Table 1.

Relative signal intensities at each cell pole were determined from 3D-maximum projections using ImageJ software and were calculated by normalising the cortex-associated fluorescent signal at the semi-hemispheres at either end of the longitudinal axis of the cell, either against a comparably sized area of non-polar cytoplasm, or a comparably sized area of image background. Average relative signal intensities and standard deviations (summarised in Table 2) were generated using data from more than 50 cells.

We thank Colin Gordon (University of Edinburgh), Keith Gull (University of Oxford), William Gullick (University of Kent), Iain Hagan (University of Manchester), Sergio Moreno and Yolanda Sánchez (University of Salamanca) and Viesturs Simanis (University of Lausanne) for strains and reagents. We thank Colin Gordon for suggestions and discussions during early stages of the project. We thank Sheran Attanapola, Stan Burgess, Campbell Gourlay, Janni Petersen and Xin Xiang for comments upon the manuscript. This work was funded by Ramón Areces and BBSRC David Phillips fellowships to R.M.-G. and D.P.M., respectively.

References

Bahler, J., Wu, J. Q., Longtine, M. S., Shah, N. G., McKenzie, A., 3rd, Steever, A. B., Wach, A., Philippsen, P. and Pringle, J. R. (1998). Heterologous modules for efficient and versatile PCR-based gene targeting in Schizosaccharomyces pombe. *Yeast* **14**, 943-951.

Beinhauer, J. D., Hagan, I. M., Hegemann, J. H. and Fleig, U. (1997). Mal3, the fission yeast homologue of the human APC-interacting protein EB-1 is required for microtubule integrity and the maintenance of cell form. *J. Cell Biol.* **139**, 717-728.

Benito, J., Martin-Castellanos, C. and Moreno, S. (1998). Regulation of the G1 phase of the cell cycle by periodic stabilization and degradation of the p25rum1 CDK inhibitor. *EMBO J.* **17**, 482-497.

Bratman, S. V. and Chang, F. (2007). Stabilization of overlapping microtubules by fission yeast CLASP. *Dev. Cell* **13**, 812-827.

Browning, H., Hayles, J., Mata, J., Aveline, L., Nurse, P. and McIntosh, J. R. (2000). Tea2p is a kinesin-like protein required to generate polarized growth in fission yeast. *J. Cell Biol.* **151**, 15-28.

Brunner, D. and Nurse, P. (2000). CLIP170-like tip1p spatially organizes microtubular dynamics in fission yeast. *Cell* **102**, 695-704.

Busch, K. E. and Brunner, D. (2004). The microtubule plus end-tracking proteins mal3p and tip1p cooperate for cell-end targeting of interphase microtubules. *Curr. Biol.* **14**, 548-559.

David, D. C., Layfield, R., Serpell, L., Narain, Y., Goedert, M. and Spillantini, M. G. (2002). Proteasomal degradation of tau protein. *J. Neurochem.* **83**, 176-185.

Dragestein, K. A., van Cappellen, W. A., van Haren, J., Tsibidis, G. D., Akhmanova, A., Knoch, T. A., Grosveld, F. and Galjart, N. (2008). Dynamic behavior of GFP-CLIP-170 reveals fast protein turnover on microtubule plus ends. *J. Cell Biol.* **180**, 729-737.

Drubin, D. G. and Nelson, W. J. (1996). Origins of cell polarity. *Cell* **84**, 335-344.

Elsasser, S. and Finley, D. (2005). Delivery of ubiquitinated substrates to protein-unfolding machines. *Nat. Cell Biol.* **7**, 742-749.

Eng, K., Naqvi, N. I., Wong, K. C. and Balasubramanian, M. K. (1998). Rng2p, a protein required for cytokinesis in fission yeast, is a component of the actomyosin ring and the spindle pole body. *Curr. Biol.* **8**, 611-621.

Fujita-Becker, S., Tsiavaliaris, G., Ohkura, R., Shimada, T., Manstein, D. J. and Sutoh, K. (2006). Functional characterization of the N-terminal region of myosin-2. *J. Biol. Chem.* **281**, 36102-36109.

Fukata, M., Watanabe, T., Noritake, J., Nakagawa, M., Yamaga, M., Kuroda, S., Matsuura, Y., Iwamatsu, A., Perez, F. and Kaibuchi, K. (2002). Rac1 and Cdc42 capture microtubules through IQGAP1 and CLIP-170. *Cell* **109**, 873-885.

Goode, B. L., Drubin, D. G. and Barnes, G. (2000). Functional cooperation between the microtubule and actin cytoskeletons. *Curr. Opin. Cell Biol.* **12**, 63-71.

Gordon, C., McGurk, G., Wallace, M. and Hastie, N. D. (1996). A conditional lethal mutant in the fission yeast 26 S protease subunit mts3+ is defective in metaphase to anaphase transition. *J. Biol. Chem.* **271**, 5704-5711.

Grallert, A., Beuter, C., Craven, R. A., Bagley, S., Wilks, D., Fleig, U. and Hagan, I. M. (2006). S. pombe CLASP needs dynein, not EB1 or CLIP170, to induce microtubule instability and slows polymerization rates at cell tips in a dynein-dependent manner. *Genes Dev.* **20**, 2421-2436.

Grallert, A., Martin-Garcia, R., Bagley, S. and Mulvihill, D. P. (2007). In vivo movement of the type V myosin Myo52 requires dimerisation but is independent of the neck domain. *J. Cell Sci.* **120**, 4093-4098.

Hagan, I. M. and Hyams, J. S. (1988). The use of cell division cycle mutants to investigate the control of microtubule distribution in the fission yeast Schizosaccharomyces pombe. *J. Cell Sci.* **89**, 343-357.

Harlow, E. and Lane, D. (1988). *Antibodies: A Laboratory Manual*. Cold Spring Harbor, NY: Cold Spring Harbor Laboratory Press.

Hartmann-Petersen, R., Hendil, K. B. and Gordon, C. (2003a). Ubiquitin binding proteins protect ubiquitin conjugates from disassembly. *FEBS Lett.* **535**, 77-81.

Hartmann-Petersen, R., Seeger, M. and Gordon, C. (2003b). Transferring substrates to the 26S proteasome. *Trends Biochem. Sci.* **28**, 26-31.

Hayles, J. and Nurse, P. (2001). A journey into space. *Nat. Rev. Mol. Cell Biol.* **2**, 647-656.

He, X., Jones, M. H., Winey, M. and Sazer, S. (1998). Mph1, a member of the Mps1-like family of dual specificity protein kinases, is required for the spindle checkpoint in S. pombe. *J. Cell Sci.* **111**, 1635-1647.

Hitchcock, A. L., Auld, K., Gygi, S. P. and Silver, P. A. (2003). A subset of membrane-associated proteins is ubiquitinated in response to mutations in the endoplasmic reticulum degradation machinery. *Proc. Natl. Acad. Sci. USA* **100**, 12735-12740.

Hwang, E., Kusch, J., Barral, Y. and Huffaker, T. C. (2003). Spindle orientation in Saccharomyces cerevisiae depends on the transport of microtubule ends along polarized actin cables. *J. Cell Biol.* **161**, 483-488.

Iioka, H., Iemura, S., Natsume, T. and Kinoshita, N. (2007). Wnt signalling regulates paxillin ubiquitination essential for mesodermal cell motility. *Nat. Cell Biol.* **9**, 813-821.

Kang, Y., Vossler, R. A., Diaz-Martinez, L. A., Winter, N. S., Clarke, D. J. and Walters, K. J. (2006). UBL/UBA ubiquitin receptor proteins bind a common tetraubiquitin chain. *J. Mol. Biol.* **356**, 1027-1035.

Kawasaki, Y., Sato, R. and Akiyama, T. (2003). Mutated APC and Asef are involved in the migration of colorectal tumour cells. *Nat. Cell Biol.* **5**, 211-215.

Lantz, V. A. and Miller, K. G. (1998). A class VI unconventional myosin is associated with a homologue of a microtubule-binding protein, cytoplasmic linker protein-170, in neurons and at the posterior pole of Drosophila embryos. *J. Cell Biol.* **140**, 897-910.

MacIver, F. H., Glover, D. M. and Hagan, I. M. (2003). A 'marker switch' approach for targeted mutagenesis of genes in Schizosaccharomyces pombe. *Yeast* **20**, 587-594.

Marks, J., Hagan, I. M. and Hyams, J. S. (1986). Growth polarity and cytokinesis in fission yeast: the role of the cytoskeleton. *J. Cell Sci. Suppl.* **5**, 229-241.

Martin, S. G., McDonald, W. H., Yates, J. R., 3rd and Chang, F. (2005). Tea4p links microtubule plus ends with the formin for3p in the establishment of cell polarity. *Dev. Cell* **8**, 479-491.

Mata, J. and Nurse, P. (1997). tea1 and the microtubular cytoskeleton are important for generating global spatial order within the fission yeast cell. *Cell* **89**, 939-949.

Mehta, A. D., Rock, R. S., Rief, M., Spudich, J. A., Mooseker, M. S. and Cheney, R. E. (1999). Myosin-V is a processive actin-based motor. *Nature* **400**, 590-593.

Mitchison, J. M. and Nurse, P. (1985). Growth in cell length in the fission yeast Schizosaccharomyces pombe. *J. Cell Sci.* **75**, 357-376.

Moreno, S., Klar, A. and Nurse, P. (1991). Molecular genetic analysis of fission yeast Schizosaccharomyces pombe. *Methods Enzymol.* **194**, 795-823.

Motegi, F., Arai, R. and Mabuchi, I. (2001). Identification of two type V myosins in fission yeast, one of which functions in polarized cell growth and moves rapidly in the cell. *Mol. Biol. Cell* **12**, 1367-1380.

Mulvihill, D. P., Edwards, S. R. and Hyams, J. S. (2006). A critical role for the type V myosin, Myo52, in septum deposition and cell fission during cytokinesis in Schizosaccharomyces pombe. *Cell Motil. Cytoskeleton* **63**, 149-161.

Pardo, M. and Nurse, P. (2005). The nuclear rim protein Amo1 is required for proper microtubule cytoskeleton organisation in fission yeast. *J. Cell Sci.* **118**, 1705-1714.

Peth, A., Boettcher, J. P. and Dubiel, W. (2007). Ubiquitin-dependent proteolysis of the microtubule end-binding protein 1, EB1, is controlled by the COP9 signalosome: possible consequences for microtubule filament stability. *J. Mol. Biol.* **368**, 550-563.

Rao, H. and Sastry, A. (2002). Recognition of specific ubiquitin conjugates is important for the proteolytic functions of the ubiquitin-associated domain proteins Dsk2 and Rad23. *J. Biol. Chem.* **277**, 11691-11695.

Reed, S. I. (2003). Ratchets and clocks: the cell cycle, ubiquitylation and protein turnover. *Nat. Rev. Mol. Cell Biol.* **4**, 855-864.

Reed, S. I. (2006). The ubiquitin-proteasome pathway in cell cycle control. *Results Probl. Cell Differ.* **42**, 147-181.

Rickard, J. E. and Kreis, T. E. (1991). Binding of pp170 to microtubules is regulated by phosphorylation. *J. Biol. Chem.* **266**, 17597-17605.

Sawin, K. E. and Nurse, P. (1998). Regulation of cell polarity by microtubules in fission yeast. *J. Cell Biol.* **142**, 457-471.

Simanis, V. and Nurse, P. (1986). The cell cycle control gene cdc2+ of fission yeast encodes a protein kinase potentially regulated by phosphorylation. *Cell* **45**, 261-268.

Solomon, F. and Zurn, A. (1981). The cytoskeleton and specification of neuronal morphology. *Neurosci. Res. Program Bull.* **19**, 100-124.

Tatebe, H., Shimada, K., Uzawa, S., Morigasaki, S. and Shiozaki, K. (2005). Wsh3/Tea4 is a novel cell-end factor essential for bipolar distribution of Tea1 and protects cell polarity under environmental stress in S. pombe. *Curr. Biol.* **15**, 1006-1015.

Verde, F., Mata, J. and Nurse, P. (1995). Fission yeast cell morphogenesis: identification of new genes and analysis of their role during the cell cycle. *J. Cell Biol.* **131**, 1529-1538.

Wen, Y., Eng, C. H., Schmoranzer, J., Cabrera-Poch, N., Morris, E. J., Chen, M., Wallar, B. J., Alberts, A. S. and Gundersen, G. G. (2004). EB1 and APC bind to mDia to stabilize microtubules downstream of Rho and promote cell migration. *Nat. Cell Biol.* **6**, 820-830.

Wilkinson, C. R., Wallace, M., Morphew, M., Perry, P., Allshire, R., Javerzat, J. P., McIntosh, J. R. and Gordon, C. (1998). Localization of the 26S proteasome during mitosis and meiosis in fission yeast. *EMBO J.* **17**, 6465-6476.

Wilkinson, C. R., Seeger, M., Hartmann-Petersen, R., Stone, M., Wallace, M., Semple, C. and Gordon, C. (2001). Proteins containing the UBA domain are able to bind to multi-ubiquitin chains. *Nat. Cell Biol.* **3**, 939-943.

Win, T. Z., Gachet, Y., Mulvihill, D. P., May, K. M. and Hyams, J. S. (2001). Two type V myosins with non-overlapping functions in the fission yeast Schizosaccharomyces pombe: Myo52 is concerned with growth polarity and cytokinesis, Myo51 is a component of the cytokinetic actin ring. *J. Cell Sci.* **114**, 69-79.

Wu, X. S., Tsan, G. L. and Hammer, J. A., 3rd (2005). Melanophilin and myosin Va track the microtubule plus end on EB1. *J. Cell Biol.* **171**, 201-207.

Yin, H., Pruyne, D., Huffaker, T. C. and Bretscher, A. (2000). Myosin V orientates the mitotic spindle in yeast. *Nature* **406**, 1013-1015.

Zimmerman, S. and Chang, F. (2005). Effects of {gamma}-tubulin complex proteins on microtubule nucleation and catastrophe in fission yeast. *Mol. Biol. Cell* **16**, 2719-2733.